Available online at www.sciencedirect.com
SCIENCE DIRECT®
International Journal of Heat and Mass Transfer 47 (2004) 4449–4457
International Journal of HEAT and MASS TRANSFER
www.elsevier.com/locate/ijhmt

Finite difference analysis of unsteady natural convection MHD flow past an inclined plate with variable surface heat and mass flux

P. Ganesan [a,*], G. Palani [b]

[a] Department of Mathematics, Anna University, Chennai 600025, India
[b] #5 (New No. 19) 4th Street, Rajaji Nagar, Villivakkam, Chennai 600 049, India

Received 29 August 2003; received in revised form 2 February 2004
Available online 3 July 2004

Abstract

A numerical solution of the transient free convection MHD flow of an incompressible viscous fluid past a semi-infinite inclined plate with variable surface heat and mass flux is presented here. The non-dimensional governing equations of the flow are unsteady, coupled and non-linear integro partial differential equations. The governing equations are solved by an efficient, more accurate and unconditionally stable implicit finite difference scheme. Velocity, temperature and concentration of the flow have been presented for various parameters such as Prandtl number, Schmidt number, the buoyancy ratio parameter, Grashof number, inclination angle ϕ and the magnetic parameter. The local and average skin friction, Nusselt number and Sherwood number are also presented graphically.

Keywords: Convection; Finite difference; Inclined plate; Magnetic parameter; Prandtl number; Skin friction

1. Introduction

Natural convection is frequently encountered in our environment and engineering devices. Free convection flow is caused by the temperature difference and also the flow is affected by the difference in concentration of material constitution. Quite often one can observe that both heat and mass transfer occur simultaneously in free convection. This study of flow phenomena has a wide range of applications in the field of science and technology.

Gebhart and Pera [1] observed the steady state natural convection on a vertical plate with variable surface temperature and variable mass diffusion. Using similarity variables they solved the boundary layer equations. Callahan and Marner [2] solved the problem of transient free convection with mass transfer on an isothermal vertical plate by using an explicit finite difference scheme. Soundalgekar and Ganesan [3] have solved the problem for transient free convection with mass transfer on a vertical plate with constant heat flux by using an implicit finite difference scheme. Ekambavannan and Ganesan [4] studied the problem of transient natural convection flows over an inclined plate with variable surface temperature and mass diffusion. Ganesan and Palani [5] have analysed numerically for transient free convection flow past a semi-infinite inclined plate with variable surface heat and mass flux.

The study of magnetohydrodynamics plays an important role in agriculture, engineering and petroleum industries. The problem of free convection under the influence of a magnetic field has attracted the interest of many researchers in view of its applications in geophysics and astrophysics. The problem under consideration has important applications in the study of geophysical formulations; in the explorations and

* Corresponding author. Tel.: +91-44-22203300; fax: +91-44-22201800.
E-mail addresses: ganesan@annauniv.edu (P. Ganesan), gpalani32@yahoo.co.in (G. Palani).

0017-9310/$ - see front matter © 2004 Published by Elsevier Ltd.
doi:10.1016/j.ijheatmasstransfer.2004.04.034

Nomenclature

a	constant
b	constant
B_0	magnetic field strength
C'	species concentration
C	dimensionless species concentration
D	coefficient of diffusion in the mixture
Gr	thermal Grashof number
Gc	mass Grashof number
g	acceleration due to gravity
k	thermal conductivity
M	magnetic parameter
m	exponent in the power law variation of the mass flux
N	combined buoyancy ratio parameter
$\overline{Nu}$	dimensionless average Nusselt number
Nu_X	dimensionless local Nusselt number
n	exponent in power law variation of the heat flux
Pr	Prandtl number
Sc	Schmidt number
$\overline{Sh}$	dimensionless average Sherwood number
Sh_X	dimensionless local Sherwood number
T'	temperature
T	dimensionless temperature
t'	time
t	dimensionless time
u, v	velocity components in x-, y-directions, respectively
U, V	dimensionless velocity components in X-, Y-directions, respectively
x	spatial coordinate along the plate
X	dimensionless spatial coordinate
y	spatial coordinate along upward normal to the plate
Y	dimensionless spatial coordinate along upward normal to the plate

Greek symbols

α	thermal diffusivity
β	volumetric coefficient of thermal expansion
β^*	volumetric coefficient of expansion with concentration
ϕ	angle of inclination of the plate with the horizontal
σ	electrical conductivity
ν	kinematic viscosity
ρ	density
τ_X	dimensionless local skin friction
$\bar{\tau}$	dimensionless average skin friction

Subscripts

i	designates grid point along the X-direction
j	designates grid point along the Y-direction
w	conditions on the wall
∞	free stream condition

Superscript

k	time step level

thermal recovery of oil; and in the underground nuclear waste storage sites. Magnetohydrodynamics has its own practical applications too. For instance, it may be used to deal with problems such as cooling of nuclear reactors by liquid sodium and induction flow meter, which depends on the potential difference in the fluid in the direction perpendicular to the motion and to the magnetic field.

Soundalgekar et al. [6] analysed the problem of free convection effects on Stokes problem for a vertical plate under the action of transversely applied magnetic field. Sacheti et al. [7] obtained an exact solution for unsteady magnetohydrodynamics free convection flow on an impulsively started vertical plate with constant heat flux. Shanker and Kishan [8] discussed the effect of mass transfer on the MHD flow past an impulsively started vertical plate with variable temperature or constant heat flux. Elbashbeshy [9] studied heat and mass transfer along a vertical plate under the combined buoyancy effects of thermal and species diffusion, in the presence of the magnetic field. Helmy [10] presented an unsteady two-dimensional laminar free convection flow of an incompressible, viscous electrically conducting (Newtonian or polar) fluid through a porous medium bounded by an infinite vertical plane surface of constant temperature. Takhar et al. [11] developed to study the unsteady mixed convection flow over a vertical cone rotating in an ambient fluid with a time-dependent angular velocity in the presence of a magnetic field. The coupled non-linear partial differential equations governing the flow have been solved numerically using an implicit finite-difference scheme. Ganesan and Palani [12] studied the effects of the MHD on the two-dimensional free convective flow of a viscous incompressible fluid past a semi-infinite isothermal vertical plate. The dimensionless governing equations are unsteady, two-dimensional, coupled and non-linear are solved numerically using an implicit finite difference scheme.

In recent years, the effects of the transverse magnetic field on the flow of an incompressible, viscous electrically conducting fluid have also been studied extensively by many research workers. However, unsteady natural convection flow over an inclined plate with MHD has not been given any attention in the literature. Hence

now we propose to study the problem of unsteady natural convection flow of a viscous incompressible electrically conducting fluid past an inclined plate with variable heat and mass flux, under the influence of magnetic field.

2. Mathematical formulation

A problem of two-dimensional, unsteady, laminar free convection flow past a semi-infinite inclined plate of a viscous incompressible electrically conducting fluid with variable surface heat and mass flux under the influence of transversely applied magnetic field is formulated mathematically in this section. It is assumed that the concentration C' of the diffusing species in the binary mixture is very small in comparison to other chemical species, which are present. This leads to the assumption that the Soret and Dufor effects are negligible. It is also assumed that the effect of viscous dissipation is negligible in the energy equation and there is no chemical reaction between the fluid and the diffusing species. A uniformly transverse magnetic field is applied in the direction of flow. It is further assumed that the interaction of the induced magnetic field with the flow is considered to be negligible compared to the interaction of the applied magnetic field with the flow.

The angle of inclination of the plate with the horizontal is assumed to be ϕ. The x-axis is measured along the plate and y-axis is taken along upward normal to the plate. Initially, it is assumed that the plate and the fluid are of the same temperature and concentration. The heat and mass is supplied from the plate to the fluid at a rate of $q_w(x) = ax^n$ and $q_w^*(x) = bx^m$, respectively, and both are maintained at the same level for all time $t' > 0$. Then under these assumptions, the governing boundary layer equations of mass, momentum, energy and species concentration for free convection flows with Boussinesq's approximation are as follows:

$$\frac{\partial u}{\partial x} + \frac{\partial v}{\partial y} = 0 \tag{1}$$

$$\begin{aligned}\frac{\partial u}{\partial t'} + u\frac{\partial u}{\partial x} + v\frac{\partial u}{\partial y} &= g\beta\cos\phi\frac{\partial}{\partial x}\int_y^\infty (T' - T'_\infty)\,\mathrm{d}y \\ &\quad + g\beta^*\cos\phi\frac{\partial}{\partial x}\int_y^\infty (C' - C'_\infty)\,\mathrm{d}y \\ &\quad + g\beta\sin\phi(T' - T'_\infty) + g\beta^*\sin\phi(C' - C'_\infty) \\ &\quad + \nu\frac{\partial^2 u}{\partial y^2} - \frac{\sigma B_0^2}{\rho}u\end{aligned} \tag{2}$$

$$\frac{\partial T'}{\partial t'} + u\frac{\partial T'}{\partial x} + v\frac{\partial T'}{\partial y} = \alpha\frac{\partial^2 T'}{\partial y^2} \tag{3}$$

$$\frac{\partial C'}{\partial t'} + u\frac{\partial C'}{\partial x} + v\frac{\partial C'}{\partial y} = D\frac{\partial^2 C'}{\partial y^2} \tag{4}$$

The initial and boundary conditions are

$$\begin{aligned}&t' \leqslant 0 : u = 0, \quad v = 0, \quad T' = T'_\infty, C' = C'_\infty \\ &t' > 0 : u = 0, \quad v = 0 \\ &\frac{\partial T'}{\partial y} = -\frac{q_w(x)}{k}, \quad \frac{\partial C'}{\partial y} = -\frac{q_w^*(x)}{D} \quad \text{at } y = 0 \\ &u = 0, \quad T' = T'_\infty, \quad C' = C'_\infty \quad \text{at } x = 0 \\ &u \to 0, \quad T' \to T'_\infty, \quad C' \to C'_\infty \quad \text{as } y \to \infty\end{aligned} \tag{5}$$

where $q_w(x) = ax^n$, $q_w^*(x) = bx^m$.

Introducing the following non-dimensional quantities

$$\begin{aligned}&X = \frac{x}{L}, \quad Y = \frac{y}{L}Gr^{1/4}, \quad U = \frac{uL}{\nu}Gr^{-1/2} \\ &V = \frac{vL}{\nu}Gr^{-1/4}, \quad t = \frac{\nu t'}{L^2}Gr^{1/2}, \quad M = \frac{\sigma B_0^2 L^2}{\rho\nu}Gr^{-1/2} \\ &T = \frac{(T' - T'_\infty)}{[q_w(L)L/k]}Gr^{1/4}, \quad C = \frac{(C' - C'_\infty)}{[q_w^*(L)L/D]}Gr^{1/4} \\ &Gr = \frac{g\beta L^4 q_w(L)}{\nu^2 k}, \quad Gc = \frac{g\beta^* L^4 q_w^*(L)}{\nu^2 D} \\ &Pr = \frac{\nu}{\alpha}, \quad Sc = \frac{\nu}{D}, \quad N = \frac{Gc}{Gr}\end{aligned} \tag{6}$$

Eqs. (1)–(4) are reduced to the following non-dimensional form.

$$\frac{\partial U}{\partial X} + \frac{\partial V}{\partial Y} = 0 \tag{7}$$

$$\begin{aligned}\frac{\partial U}{\partial t} + U\frac{\partial U}{\partial X} + V\frac{\partial U}{\partial Y} &= Gr^{-1/2}\cos\phi\frac{\partial}{\partial X}\int_Y^\infty T\,\mathrm{d}Y \\ &\quad + NGr^{-1/2}\cos\phi\frac{\partial}{\partial X}\int_Y^\infty C\,\mathrm{d}Y \\ &\quad + Gr^{-1/4}T\sin\phi + NGr^{-1/4}C\sin\phi \\ &\quad + \frac{\partial^2 U}{\partial Y^2} - MU\end{aligned} \tag{8}$$

$$\frac{\partial T}{\partial t} + U\frac{\partial T}{\partial X} + V\frac{\partial T}{\partial Y} = \frac{1}{Pr}\frac{\partial^2 T}{\partial Y^2} \tag{9}$$

$$\frac{\partial C}{\partial t} + U\frac{\partial C}{\partial X} + V\frac{\partial C}{\partial Y} = \frac{1}{Sc}\frac{\partial^2 C}{\partial Y^2} \tag{10}$$

The corresponding initial and boundary conditions in non-dimensional quantities are given by

$$\begin{aligned}&t \leqslant 0 : U = 0, \quad V = 0, \quad T = 0, \quad C = 0 \\ &t > 0 : U = 0, \quad V = 0 \\ &\frac{\partial T}{\partial Y} = -X^n, \quad \frac{\partial C}{\partial Y} = -X^m \quad \text{at } Y = 0 \\ &U = 0, \quad T = 0, \quad C = 0 \quad \text{at } X = 0 \\ &U \to 0, \quad T \to 0, \quad C \to 0 \quad \text{as } Y \to \infty\end{aligned} \tag{11}$$

Local and average skin friction, Nusselt number and Sherwood number. In non-dimensional quantities are

$$\tau_X = Gr^{3/4}\left(\frac{\partial U}{\partial Y}\right)_{Y=0} \tag{12}$$

$$\bar{\tau} = Gr^{3/4}\int_0^1 \left[\frac{\partial U}{\partial Y}\right]_{Y=0} \mathrm{d}X \tag{13}$$

$$Nu_X = -XGr^{1/4}\left(\frac{\partial T}{\partial Y}\right)_{Y=0}\Big/ T_{Y=0} \tag{14}$$

$$\overline{Nu} = -Gr^{1/4}\int_0^1 \left[\left(\frac{\partial T}{\partial Y}\right)_{Y=0}\Big/ T_{Y=0}\right]\mathrm{d}X \tag{15}$$

$$Sh_X = -XGr^{1/4}\left(\frac{\partial C}{\partial Y}\right)_{Y=0}\Big/ C_{Y=0} \tag{16}$$

$$\overline{Sh} = -Gr^{1/4}\int_0^1 \left[\left(\frac{\partial C}{\partial Y}\right)_{Y=0}\Big/ C_{Y=0}\right]\mathrm{d}X \tag{17}$$

3. Numerical technique

The unsteady, non-linear, coupled and integro partial differential equations (7)–(10) with the initial and boundary conditions (11) are solved by employing a finite difference scheme of Crank–Nicolson type.

The finite-difference equation corresponding to Eqs. (7)–(10) is given by

$$\frac{U^{k+1}_{i,j-1} - U^{k+1}_{i-1,j-1} + U^{k+1}_{i,j} - U^{k+1}_{i-1,j} + U^{k}_{i,j-1} - U^{k}_{i-1,j-1} + U^{k}_{i,j} - U^{k}_{i-1,j}}{4\Delta X} + \frac{V^{k+1}_{i,j} - V^{k+1}_{i,j-1} + V^{k}_{i,j} - V^{k}_{i,j-1}}{2\Delta Y} = 0 \tag{18}$$

$$\begin{aligned}
&\frac{U^{k+1}_{i,j} - U^{k}_{i,j}}{\Delta t} + U^{k}_{i,j}\frac{\left(U^{k+1}_{i,j} - U^{k+1}_{i-1,j} + U^{k}_{i,j} - U^{k}_{i-1,j}\right)}{2\Delta X} \\
&\quad + V^{k}_{i,j}\frac{\left(U^{k+1}_{i,j+1} - U^{k+1}_{i,j-1} + U^{k}_{i,j+1} - U^{k}_{i,j-1}\right)}{4\Delta Y} \\
&\quad = Gr^{-1/2}\cos\phi\frac{\partial}{\partial X}\int_Y^\infty T\,\mathrm{d}Y + NGr^{-1/2}\cos\phi\frac{\partial}{\partial X} \\
&\qquad \times \int_Y^\infty C\,\mathrm{d}Y + Gr^{-1/4}\sin\phi\frac{\left[T^{k+1}_{i,j} + T^{k}_{i,j}\right]}{2} \\
&\qquad + NGr^{-1/4}\sin\phi\frac{\left[C^{k+1}_{i,j} + C^{k}_{i,j}\right]}{2} \\
&\qquad + \frac{\left(U^{k+1}_{i,j-1} - 2U^{k+1}_{i,j} + U^{k+1}_{i,j+1} + U^{k}_{i,j-1} - 2U^{k}_{i,j} + U^{k}_{i,j+1}\right)}{2(\Delta Y)^2} \\
&\qquad - M\frac{(U^{k+1}_{i,j} + U^{k}_{i,j})}{2}
\end{aligned} \tag{19}$$

$$\begin{aligned}
&\frac{T^{k+1}_{i,j} - T^{k}_{i,j}}{\Delta t} + U^{k}_{i,j}\frac{\left(T^{k+1}_{i,j} - T^{k+1}_{i-1,j} + T^{k}_{i,j} - T^{k}_{i-1,j}\right)}{2\Delta X} \\
&\quad + V^{k}_{i,j}\frac{\left(T^{k+1}_{i,j+1} - T^{k+1}_{i,j-1} + T^{k}_{i,j+1} - T^{k}_{i,j-1}\right)}{4\Delta Y} \\
&\quad = \frac{\left(T^{k+1}_{i,j-1} - 2T^{k+1}_{i,j} + T^{k+1}_{i,j+1} + T^{k}_{i,j-1} - 2T^{k}_{i,j} + T^{k}_{i,j+1}\right)}{2Pr(\Delta Y)^2}
\end{aligned} \tag{20}$$

$$\begin{aligned}
&\frac{C^{k+1}_{i,j} - C^{k}_{i,j}}{\Delta t} + U^{k}_{i,j}\frac{\left(C^{k+1}_{i,j} - C^{k+1}_{i-1,j} + C^{k}_{i,j} - C^{k}_{i-1,j}\right)}{2\Delta X} \\
&\quad + V^{k}_{i,j}\frac{\left(C^{k+1}_{i,j+1} - C^{k+1}_{i,j-1} + C^{k}_{i,j+1} - C^{k}_{i,j-1}\right)}{4\Delta Y} \\
&\quad = \frac{\left(C^{k+1}_{i,j-1} - 2C^{k+1}_{i,j} + C^{k+1}_{i,j+1} + C^{k}_{i,j-1} - 2C^{k}_{i,j} + C^{k}_{i,j+1}\right)}{2Sc(\Delta Y)^2}
\end{aligned} \tag{21}$$

The thermal condition at $Y = 0$ in the finite difference form is

$$\frac{1}{2}\frac{\left(T^{k+1}_{i,1} - T^{k+1}_{i,-1} + T^{k}_{i,1} - T^{k}_{i,-1}\right)}{2(\Delta Y)} = -(i\Delta X)^n \tag{22}$$

At $Y = 0$ (i.e., $j = 0$) Eq. (20) becomes

$$\frac{T^{k+1}_{i,0} - T^{k}_{i,0}}{\Delta t} = \frac{\left(T^{k+1}_{i,-1} - 2T^{k+1}_{i,0} + T^{k+1}_{i,1} + T^{k}_{i,-1} - 2T^{k}_{i,0} + T^{k}_{i,1}\right)}{2Pr(\Delta Y)^2} \tag{23}$$

After eliminating $T^{k+1}_{i,-1} + T^{k}_{i,-1}$ from the Eqs. (22) and (23) the following equation is obtained.

$$\frac{T^{k+1}_{i,0} - T^{k}_{i,0}}{\Delta t} = \frac{\left(T^{k+1}_{i,1} - T^{k+1}_{i,0} + T^{k}_{i,1} - T^{k}_{i,0} + 2(\Delta Y)(i\Delta X)^n\right)}{Pr(\Delta Y)^2} \tag{24}$$

The species condition at $Y = 0$ in the finite difference form is

$$\frac{1}{2}\frac{\left(C^{k+1}_{i,1} - C^{k+1}_{i,-1} + C^{k}_{i,1} - C^{k}_{i,-1}\right)}{2(\Delta Y)} = -(i\Delta X)^m \tag{25}$$

At $Y = 0$ (i.e., $j = 0$) Eq. (21) becomes

$$\frac{C^{k+1}_{i,0} - C^{k}_{i,0}}{\Delta t} = \frac{\left(C^{k+1}_{i,-1} - 2C^{k+1}_{i,0} + C^{k+1}_{i,1} + C^{k}_{i,-1} - 2C^{k}_{i,0} + C^{k}_{i,1}\right)}{2Sc(\Delta Y)^2} \tag{26}$$

After eliminating $C^{k+1}_{i,-1} + C^{k}_{i,-1}$ from the Eqs. (25) and (26), the following equation is obtained

$$\frac{C_{i,0}^{k+1}-C_{i,0}^{k}}{\Delta t}=\frac{\left(C_{i,1}^{k+1}-C_{i,0}^{k+1}+C_{i,1}^{k}-C_{i,0}^{k}+2(\Delta Y)(i\Delta X)^{m}\right)}{Sc(\Delta Y)^{2}} \tag{27}$$

Here, the subscript i-designates the grid point along the X-direction, j-along the Y-direction and the superscript k along the t-direction. During any one-time step, the coefficients $U_{i,j}^{k}$ and $V_{i,j}^{k}$ appearing in the difference equations are treated as constants. The values of U, V, T and C are known at all grid points at time $t=0$ from the initial conditions. The computations of U, V, T and C at time level $(k+1)$ using the known values at previous time level (k) are done as follows:

Eqs. (21) and (27) at every internal nodal point on a particular i-level constitute a tri-diagonal system of equations, which are solved by Thomas algorithm, described by Carnahan et al. [13]. Thus, the values of C are found at every nodal point on a particular i at $(k+1)$th time level. Similarly the values of T are calculated from Eqs. (20) and (24). Using the values of C and T at $(k+1)$th time level in the Eq. (19), the values of U at $(k+1)$th time level are found in a similar manner. Integrals in this equation are evaluated using Newton-Cotes closed integration formula. Then the values of V are calculated explicitly by using Eq. (18) at every nodal point on a particular i-level. This process is repeated for various i-levels. Thus the values of C, T, U and V are known at all grid points in the rectangular region at $(k+1)$th time level.

This process is repeated in time until steady state is reached. The steady state solution is assumed to have been reached, when the absolute differences between values of U as well as temperature T and concentration C at two consecutive time steps are less than 10^{-5} at all grid points. Computations have been carried out for different values of parameters.

The derivatives involved in Eqs. (12)–(17) are evaluated using five-point approximation formula and then the integrals are evaluated using Newton-Cotes closed integration formula.

The region of integration is considered as a rectangle with sides $X_{\max}(=1.0)$ and $Y_{\max}(=24.0)$ where $Y_{\max}$ corresponds to $Y=\infty$ which lies very well outside the momentum, thermal and concentration boundary layers. After experimenting with a few sets of mesh sizes, the mesh sizes are fixed as $\Delta X=0.05$, $\Delta Y=0.25$ and $\Delta t=0.01$. In this case, the spatial mesh sizes are reduced by 50% in one direction and then in both directions and the results are compared. It is observed that, when the mesh size is reduced by 50% in the Y-direction, the results differ in the fifth decimal place. When the mesh sizes are reduced by 50% in X-direction or in the both directions the results are comparable to three decimal places. Hence these mesh sizes are considered to be appropriate mesh sizes for calculations.

4. Results and discussion

In Fig. 1 transient velocity profiles are plotted for different values of buoyancy ratio parameter N, inclination angle ϕ and magnetic field parameter M. An increase in N leads to an increase in the velocity. This indicates that the buoyancy force due to concentration dominates in the region near the plate over thermal buoyancy force on velocity. Time taken to reach the steady state increases with the increasing value of the magnetic field parameter M. From Fig. 1, we observe that the magnetic parameter M has a retarding effect on velocity. Velocity increases steadily and reaches steady state after some time. Since the tangential component of the buoyancy force increases with ϕ and dominates in the down stream, higher velocity is experienced throughout the transient period as well as in the steady state level for a system having larges angles of inclination.

For various Schmidt number and Prandtl number, transient velocity profiles are plotted in Fig. 2. The velocity of air $(Pr=0.7)$ is always greater than velocity of water $(Pr=7.0)$ for same values of other parameters. An increase in Sc leads to a fall in the velocity. Time taken to reach the steady state increases as Pr or Sc increases.

The effects of Grashof number, magnetic field parameter M, exponent n and m on steady state velocity are shown in Fig. 3. The velocity of air $(Pr=0.7)$ decreases with increasing Grashof number. The increase in the value of n and m reduces velocity on the surface up to height of the plate $X=1.0$. Therefore velocity decreases with increasing value of n or m. It is observed that the effect of m is more than that of n on velocity.

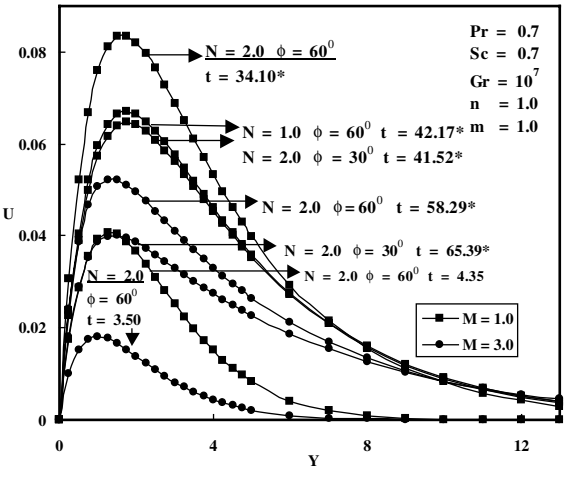

Fig. 1. Transient velocity profiles at $X=1.0$ for different N, ϕ and M (*—steady state).

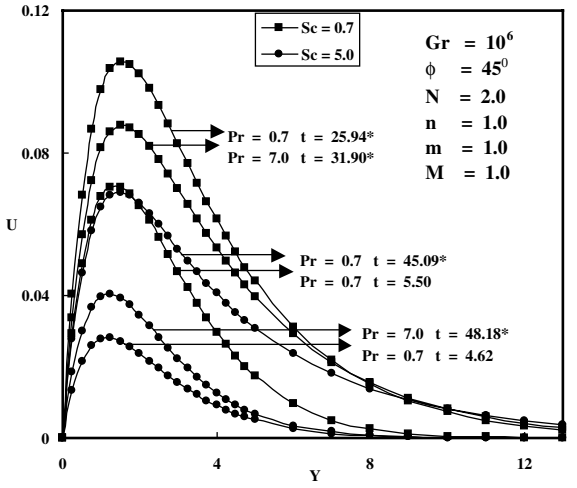

Fig. 2. Transient velocity profiles at $X = 1.0$ for different Pr and Sc (*—steady state).

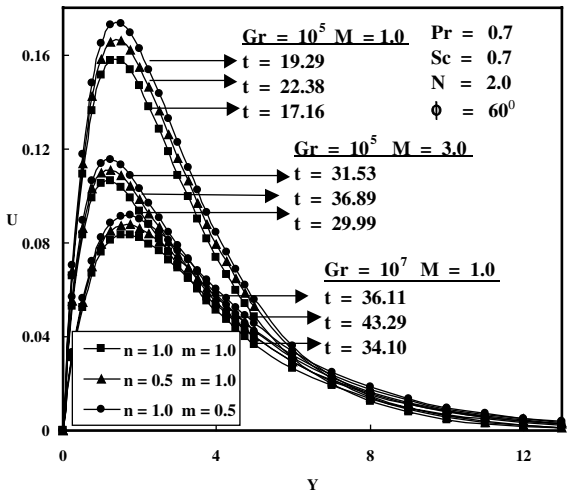

Fig. 3. Steady state velocity profiles at $X = 1.0$ for different Gr, n, m and M.

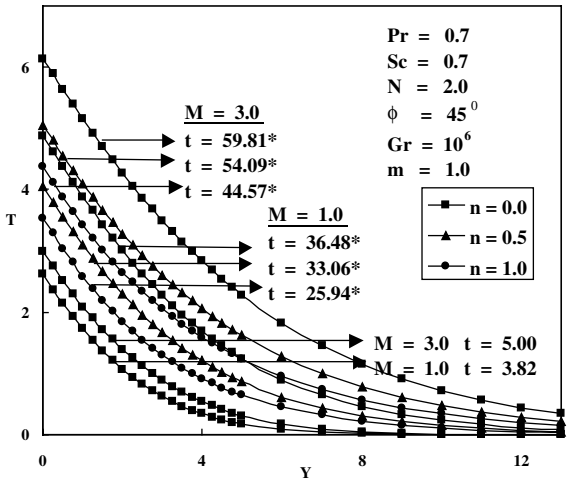

Fig. 4. Transient temperature profiles at $X = 1.0$ for different n and M (*—steady state).

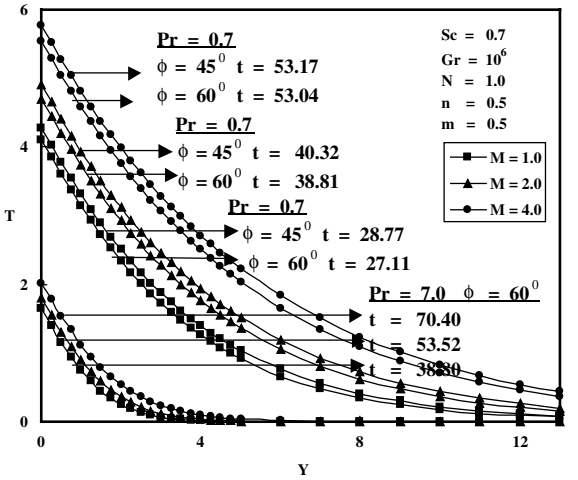

Fig. 5. Steady state temperature profiles at $X = 1.0$ for different Pr, ϕ and M.

Also it is observed that the system reaches the steady state value quickly when $n = m$.

To illustrate the effect of exponent n and magnetic parameter M on the temperature, the transient temperature distribution near the plate at $X = 1.0$ is presented in Fig. 4. Temperature increases with the increasing value of the magnetic parameter M. It is observed that the temperature decreases with increasing value of exponent n. According to the result in the above figure steady state value reaches early when $n = m$ in comparison with $n < m$. No temporal maximum is observed.

The profiles of steady state temperature for different values of Pr, ϕ and M are shown in Fig. 5. The effect of Prandtl number is very important in the temperature profiles. The thermal boundary layer thickness decreases with increasing Prandtl number. It is observed that the temperature decreases as the angle of inclination ϕ increases. Also it is observed that the system reaches steady state early when ϕ increases.

Transient concentration profiles are shown in Fig. 6 for different values of exponent m and M. Concentration reduces with increasing value of m. The concentration profile increases with the increasing value of magnetic parameter M.

In Fig. 7, Steady state concentration profiles are plotted for different values of Schmidt number, inclina-

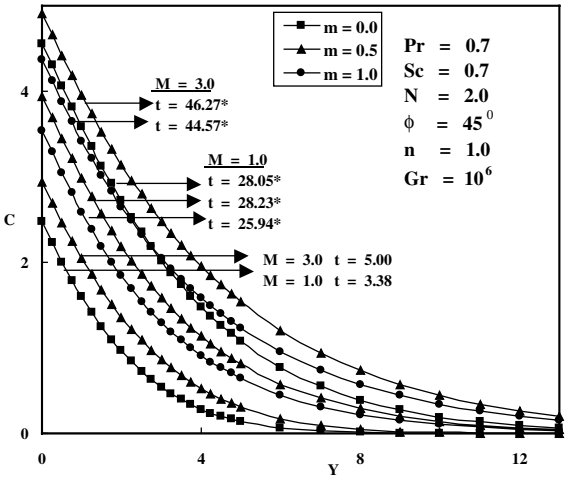

Fig. 6. Transient concentration profiles at $X = 1.0$ for different m and M (*—steady state).

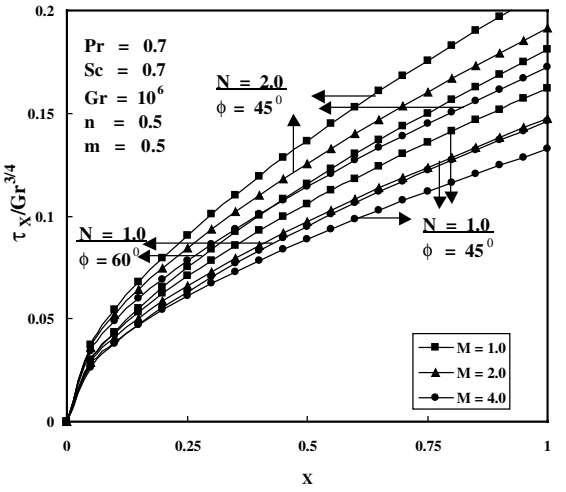

Fig. 8. Local skin friction.

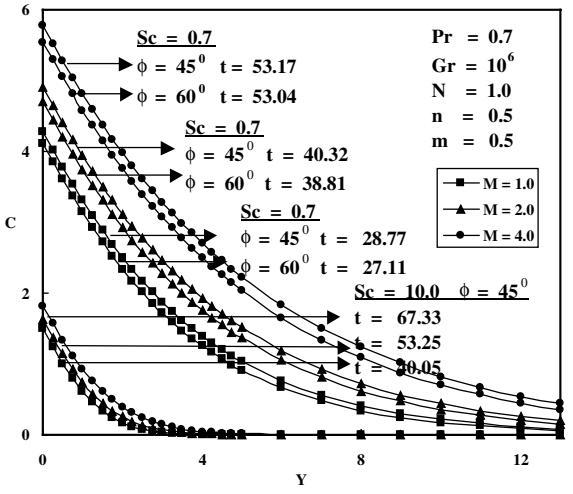

Fig. 7. Steady state concentration at $X = 1.0$ for different Sc, ϕ and M.

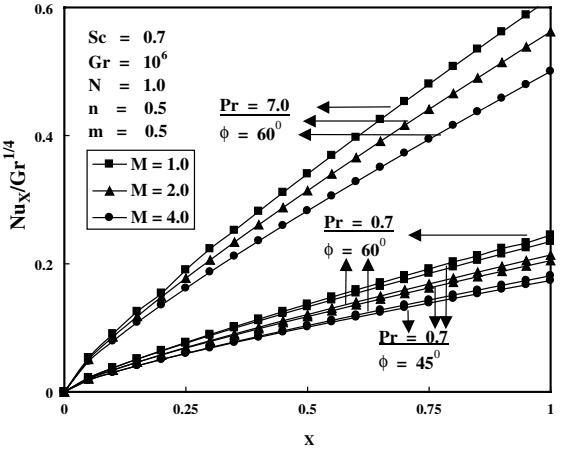

Fig. 9. Local Nusselt number.

tion angle ϕ and magnetic field parameter M. As expected concentration is lower for systems with a larger Sc or ϕ. More time is required to reach the steady state value when Sc and M are large.

In Fig. 8, values of local shear stress is plotted for various values of buoyancy ratio parameter N, ϕ and M. As the buoyancy ratio parameter N increases, local skin friction increases. The local wall shear stress decreases as M increases (or) ϕ decreases. This is because of the fact that the velocity gradient decreases near the plate as M increases (or) ϕ decreases which are shown in Fig. 1.

Local Nusselt number for different values of Pr, ϕ and M is shown in Fig. 9. It increases as X increases. The local heat transfer stronger on Pr than on the other parameters, since lower Pr gives thicker temperature profiles, which agrees with Fig. 5. Large values of Nusselt number are observed for higher value of Pr. It decreases as M increases. Also, it is observed that local Nusselt number increases by the increasing value of inclination angle ϕ.

Steady state local Sherwood number is shown in Fig. 10, for various values of Sc, ϕ and M. The effect of Sc is greater on the local Sherwood number than any other parameter. It decreases as M increases. Also it is observed that local Sherwood number decreases as ϕ decreases.

Average values of skin friction, Nusselt number and Sherwood numbers are shown in Figs. 11–13, respectively. In Fig. 11, it is observed that average skin friction

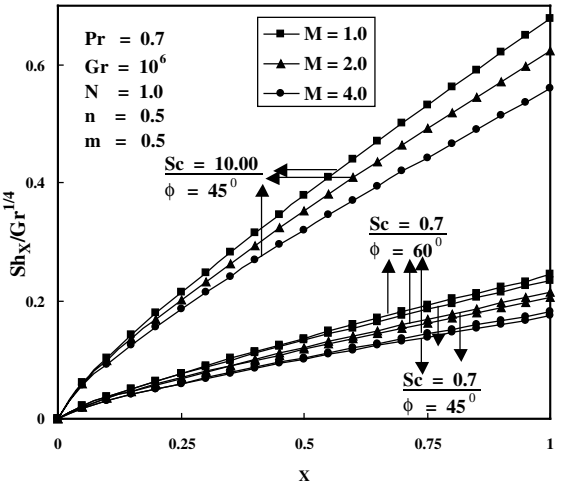

Fig. 10. Local Sherwood number.

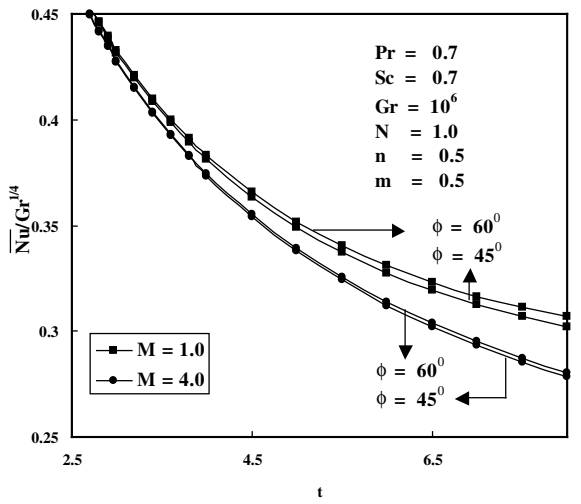

Fig. 12. Average Nusselt number.

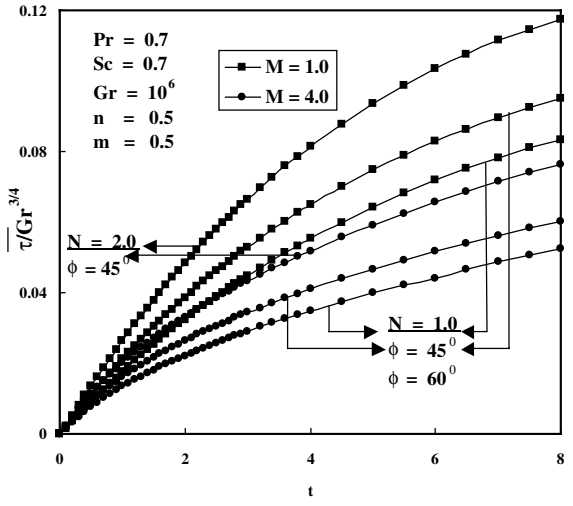

Fig. 11. Average skin friction.

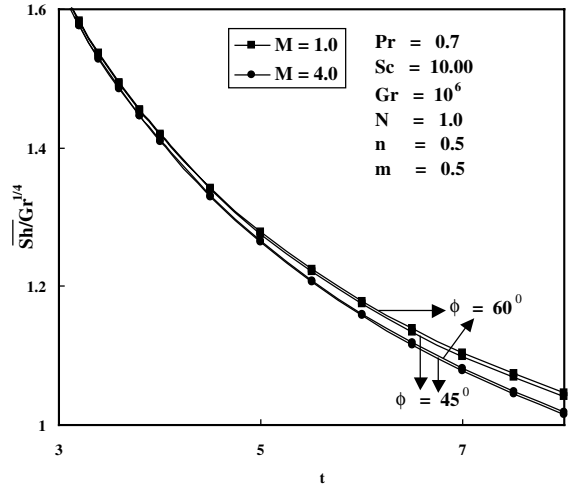

Fig. 13. Average Sherwood number.

increases with time and become steady after some time. Average skin friction gets reduced with the increasing value of M. It decreases as ϕ decreases. It is also observed that average skin friction increases as N increases.

In the initial time, higher values of average Nusselt and Sherwood numbers are observed. They decrease with time and become steady after some time. In Fig. 12, Average Nusselt numbers are presented for various values of ϕ and M. It is observed that for short times, the average Nusselt number is constant at each level for various parameters. This shows that initially there is only heat conduction. Average Nusselt number gets reduced by the increasing value of M. It decreases as ϕ decreases. In Fig. 13, Average Sherwood number is shown graphically for various values of ϕ and M. Average Sherwood number decreases as M increases. It decreases as ϕ decreases.

5. Conclusion

A detailed numerical study has been carried out for the MHD flow past a semi-infinite inclined plate with variable surface heat flux and mass flux. The dimensionless governing equations are solved by an implicit finite-difference method of Crank–Nicolson type. Conclusions of the study are as follows.

1. Time taken to reach the steady state increases with the increasing value of the magnetic field parameter.
2. The magnetic field parameter has a retarding effect on the velocity.
3. Temperature and Concentration increases with the increasing value of the magnetic field parameter.
4. Velocity increases as the angle of inclination ϕ increases throughout the transient period and steady state period.
5. In case of Sc, the velocity and concentration profiles are decreasing as Sc increases.
6. Local and average Nusselt numbers are enhanced as Pr increases.
7. Local skin friction decreases as the increasing value of magnetic field parameter M.
8. The increasing value of magnetic field parameter reduces average Nusselt number. The same trend is also noticed for average Sherwood number.

References

[1] B. Gebhart, L. Pera, The nature of vertical natural convection flows resulting from the combined buoyancy effects of thermal and mass diffusion, Int. J. Heat Mass Transfer 14 (1971) 323–329.

[2] G.D. Callahan, W.J. Marner, Transient free convection with mass transfer on an isothermal vertical flat plate, Int. J. Heat Mass Transfer 19 (1976) 165–174.

[3] V.M. Soundalgekar, P. Ganesan, Finite difference analysis of transient free convection with mass transfer on an isothermal vertical flat plate, Int. J. Eng. Sci. 19 (1981) 757–770.

[4] K. Ekambavannan, P. Ganesan, Finite difference analysis of unsteady natural convection along an inclined plate with variable surface temperature and mass diffusion, Wärme Stoffübertrag. 31 (1995) 17–24.

[5] P. Ganesan, G. Palani, Convective flow over an inclined plate with variable heat and mass flux, in: Proceedings of the Fourth ISHMT/ASME Heat and Mass transfer Conference and Fifteenth National Heat and Mass Transfer Conference, Pune, India, January 12–14, 2000, pp. 323–329.

[6] V.M. Soundalgekar, S.K. Gupta, N.S. Birajdar, Effects of mass transfer and free convection effects on MHD Stokes problem for a vertical plate, Nucl. Eng. Des. 53 (1979) 309–346.

[7] N.C. Sacheti, P. Chandran, A.K. Singh, An exact solution for unsteady magnetohydrodynamics free convection flow with constant heat flux, Int. Commun. Heat Mass Transfer 21 (1994) 131–142.

[8] B. Shanker, N. Kishan, The effects of mass transfer on the MHD flow past an impulsively started infinite vertical plate with variable temperature or constant heat flux, J. Energy, Heat Mass Transfer 19 (1997) 273–278.

[9] E.M.A. Elbashbeshy, Heat and Mass transfer along a vertical plate with variable surface tension and concentration in the presence of the magnetic field, Int. J. Eng. Sci. 34 (5) (1997) 515–522.

[10] K.A. Helmy, MHD unsteady free convection flow past a vertical porous plate, ZAMM 78 (1998) 255–270.

[11] H.S. Takhar, A.J. Chamkha, G. Nath, Unsteady mixed convection flow from a rotating vertical cone with a magnetic field, Heat and Mass Transfer 39 (2003) 297–304.

[12] P. Ganesan, G. Palani, Numerical solution of unsteady MHD flow past a semi-infinite isothermal vertical plate, in: Proceedings of the sixth ISHMT/ASME Heat and Mass Transfer Conference and Seventeenth National Heat and Mass Transfer Conference, Kalpakkam, India, January 5–7, 2004, pp. 184–187.

[13] B. Carnahan, H.A. Luther, J.O. Wilkes, Applied Numerical Methods, John Wiley and Sons, New York, 1969.